Research Communication

DMT1 as a candidate for non-transferrin-bound iron uptake in the peripheral nervous system

Rocio Martínez Vivot
Belén Goitia
Vanina Usach
Patricia C. Setton-Avruj*

Instituto de Química y Fisicoquímica Biológica (IQUIFIB), UBA-CONICET, Departamento de Química Biológica, Facultad de Farmacia y Bioquímica, Universidad de Buenos Aires, Junin 956- Buenos Aires C1113AAD, Argentina

Abstract

Iron, either in its chelated form or as holotransferrin (hTf), prevents the dedifferentiation of Schwann cells (SC), cells responsible for the myelination of the peripheral nervous system (PNS). This dedifferentiation is promoted by serum deprivation through cAMP release, PKA activation, and CREB phosphorylation. Since iron elicits its effect in a transferrin (Tf)-free environment, in this work we postulate that non-transferrin-bound iron (NTBI) uptake must be involved. Divalent metal transporter 1(DMT1) has been widely described in literature as a key player in iron metabolism, but never before in the PNS context. The presence of DMT1 was demonstrated in nerve homogenate, isolated adult-rat myelin, and cultured SC by Western Blot (WB) analysis and confirmed through its colocalization with S-100β (SC marker) by immunocytochemical and immunohistochemical analyses. Furthermore, the existence of its mRNA was verified in sciatic nerve homogenate by RT-PCR and throughout SC maturational stages. Finally, we describe DMT1's subcellular location in the plasma membrane by confocal microscopy of SC and WB of different subcellular fractions. These data allow us to suggest the participation of DMT1 as part of a Tf independent iron uptake mechanism in SC and lead us to postulate a crucial role for iron in SC maturation and, as a consequence, in PNS myelination. © 2013 BioFactors, 39(4):476–484, 2013

Keywords: *DMT1; iron; peripheral nervous system; myelination*

1. Introduction

Iron is an essential component of many enzymes and prosthetic groups, such as heme and iron- sulfur clusters [1–3], and it plays important roles in oxygen transport and storage, electron transport, and energy metabolism; it is also involved in antioxidant and beneficial prooxidant actions, as well as nonbeneficial production of reactive oxygen species (ROS), and its presence is considered essential to DNA synthesis [4–6].

Several groups have proven iron to be a crucial element in the multifactorial initiation of myelination in the central nervous system (CNS), as it is required for the biosynthesis of key components of myelin and energy production [7–9]. As oligodendrocytes (olg) strongly rely on high energy supply, iron deficiency can result in decreased olg survival and defective myelination [10,11]. Neurodegenerative diseases such as Alzheimer's disease (AD) [12]; Parkinson's disease [13], Friedreich's ataxia [14], among others [15,16] have been associated with an iron metabolism imbalance. For instance, in AD, iron accumulates more rapidly than ferritin in areas of neurodegeneration, and that accumulation occurs in the same brain regions characterized by Aβ deposition [17].

According to the World Health Organization, lack of iron is the most common nutrient deficiency in the world [18,19]. Thus the majority of neurological problems associated with iron deficiency have been attributed to hypomyelination [20,21]. In rats, a peak in brain iron uptake *in vivo* coincides with the period of greatest myelination and a shortage of iron leads to myelination deficiency [22,23]. Also during myelinogenesis, the rate of

Volume 39, Number 4, July/August 2013, Pages 476–484

**Address for correspondence to: Patricia C. Setton-Avruj*, Ph.D., Instituto de Química y Fisicoquímica Biológica (IQUIFIB), UBA-CONICET, Departamento de Química Biológica, Facultad de Farmacia y Bioquímica, Universidad de Buenos Aires, Junin 956- Buenos Aires C1113AAD, Argentina. Tel.: 54-11-49648287 Fax: 54-11-4964-5257. E-mail: setton@qb.ffyb.uba.ar.*

Received 1 October 2012; accepted 21 December 2012

Additional Supporting Information may be found in the online version of this article.

DOI: 10.1002/biof.1088

Published online 30 January 2013 in Wiley Online Library (wileyonlinelibrary.com)

uptake of transferrin (Tf) in the brain is much lower than the uptake of iron [24] strongly suggesting a NTBI uptake.

The literature reporting on the effects of iron on peripheral myelination, however, seems to be scarce and dated [25–27]. Our group has previously demonstrated that cultured Schwann cells (SC) incubated in serum-free medium become dedifferentiated and acquire a phenotype similar to SC precursors and non-myelin-forming SC. Holotransferrin (hTf) prevents the dedifferentiation promoted by serum deprivation, while apotransferrin (aTf) is unable to block this effect [28]. We have also shown that, upon treatment of SC with iron, either as NTBI or as TBI, intracellular signals towards differentiation become activated or stabilized through cAMP release, PKA activation, and CREB phosphorylation [29].

This prodifferentiating effect suggests that either iron or hTf are involved in the axonal signal that enables SC maturation and survival. Since iron elicits its effect in a transferrin (Tf)-free environment, we postulate that there must be NTBI uptake involved.

In addition to other proteins under study such as ZIP8 and ZIP14 [30], the capacity of the divalent metal transporter 1 (DMT1) to transport iron and its ubiquitous expression makes it a likely candidate for NTBI uptake in peripheral nerves. Garrick et al. have pointed out that "DMT1 has four names, transports as many as eight metals, has at least four isoforms and carries out its transport for multiple purposes" [31]. Two major functions are described in literature: one is serving as the apical iron transporter in the lumen of the gut, a function for which the isoform 1A appears to be responsible and the endosomal exit of iron into the cytosol as part of the Tf cycle; in this case evidence hints at the 1B isoform [32,33]. Both these functions (apical Fe^{2+} uptake by enterocytes and iron trafficking into cells via the Tf cycle) plus NTBI uptake into cells [34] are critical in iron homeostasis.

Considering previous results from our group which demonstrate the importance of iron in SC maturation and its prodifferentiating effect on SC in a Tf-free medium [29] we propose that DMT1 is a candidate for NTBI uptake within the peripheral nervous system (PNS).

2. Materials and Methods

2.1. Materials

Polylysine, trypsin, collagenase, cytosine arabinoside, ethidium bromide, sucrose, leupeptin, pepstatin A, Coomasie blue, bovine serum albumin, penicillin, streptomycin, Hoechst 32258, aTf, and hTf were purchased from Sigma Chem. Co (St. Louis, MO, USA). βFGF was purchased from Peprotech (Mexico). TRIZOL reagent was purchased from Invitrogen (Argentina), the RNeasy kit was purchased from QIAGEN (France), oligo-dT was purchased from Biodynamics (Argentina), M-MLV reverse transcriptase and Taq DNA polymerase were purchased from Promega. Dulbecco modified Eagle's medium (DMEM) high glucose with L-glutamine and DMEM F_{12} were acquired from GIBCO (Grand Island, NY, USA). Fetal calf serum (FCS) was purchased from Natocor (Córdoba, Argentina). PVDF membranes and ECL Plus kit were provided by Amersham-Pharmacia Biotech (UK). Ammonium ferric citrate was from Fluka Chemical (Germany). NRAMP2 (DMT1) and Na^+/K^+-ATPase β1 antibody was purchased from Santa Cruz Biotechnology Inc. (Santa Cruz, CA, USA). Secondary antibodies for immunocytochemistry, immunohistochemistry, and Western blot studies were purchased from Jackson (West Grove, PA, USA). The fluorescent mounting media was from Dako North America Inc. (Carpinteria, CA, USA). Cryoplast was purchased from Biopack (Argentina). Schwann-cell-defined medium (SCDM) is made up of DMEM F12 plus Tf 100 μg/mL, progesterone 60 ng/mL, putrescine 16 μg/mL, insulin 5 mg/L, selenium 160 ng/mL, T3 10.1 ng/mL, dexamethasone 38 ng/mL, glucose 7.9 mg/mL, BSA 300 μg/mL, penicillin 20 UI/mL, streptomicin 20 μg/mL, glutamine 2mM, HCO_3^- 1.2 g/L, which were all provided by Sigma Chem. Co (St. Louis, MO, USA).

2.2. Animals

Wistar rat embryos at embryonic day 14–20 (E14, E16, E18, and E20), newborn Wistar rat pups (2–5-days old), and adult Wistar rats (70–90-days old) were used for the experiments. All procedures with animals were performed in accordance with the guidelines of the Committee of Bioethics of Facultad de Farmacia y Bioquímica, Universidad de Buenos Aires.

2.3. Schwann Cell Cultures

2.3.1. Embryonic SC Culture.

Sciatic nerves from E14, E16, E18, and E20 rat embryos were dissected and incubated in SCDM with trypsin (0.25%) and collagenase (0.03%) for 30 Min at 37 °C. The cell suspension was centrifuged and the pellet was resuspended in SCDM + 1% FCS + βFGF 10 ng/mL. Cells were seeded at a density of 3×10^5 on polylysine-coated wells and were cultured for 3 H (E14-E18) or 24 H (E20) for RT-PCR analysis.

2.3.2. Mature SC Culture.

Sciatic nerves from 2 to 5-days-old rat pups were dissected and incubated in DMEM with trypsin (0.25%) and collagenase (0.03%) for 45 Min at 37 °C. After this period of time, the suspension was centrifuged and the medium was replaced by DMEM+10% FCS. The suspension was mechanically disrupted by passing it 10 times through a 21 g hypodermic needle and another 10 times through a 25 g needle after the enzymatic digestion. The suspension was centrifuged at 500*g* for 5 Min and the supernatant discarded. The pellet was resuspended in DMEM+10% FCS and the cells were seeded and kept for 24 H on polylysine-coated coverslips placed in multiwells (50,000 cells per well) or directly in polylysine-coated multiwells at a density of approximately 1.5×10^6 cells, for immunocytochemical studies or Western blot analysis, respectively. As previously described, culture purity obtained by this method was 95% [28].

2.4. Preparation of Subcellular Fractions

Adult Wistar rats (70–90 days) were killed by decapitation and the sciatic nerves were quickly removed, minced with scissors, and hand-homogenized with a Dounce Teflon homogenizer using 5 volumes of ice–cold 0.25 M sucrose containing 1% apoprotinin. These subcellular nerve fractions were obtained as described by an adaptation of Malviya's method [35–37]: the nuclear, the mitochondrial, the microsomal, and the plasma membrane (PM) fraction.

Centrifugation for 10 Min at 600*g* in a Sorvall SS 24 rotor generated the pellet corresponding to the nuclear fraction. After centrifugation of the supernatant for 42 Min at 20,000*g*, again in a Sorvall SS 24 rotor, the pellet was retained as the mitochondrial fraction. The PM fraction was pelleted for 20 Min at 15,000*g* in a L8-Beckman 50 Ti rotor. The microsomal fraction was obtained after centrifuging the previous supernatant for 60 Min at 105,000*g* in a L8-Beckman 50 Ti rotor.

2.5. Isolation of Peripheral Nerve Myelin

Purified myelin was obtained from sciatic nerves of adult rats by homogenizing the tissue in 2 mL of 0.32 M sucrose containing 1.1 μM leupeptin and 1.02 μM pepstatin A, in glass-Teflon homogenizer at 3000–5000 rpm. Subcellular fractionation was carried out by a modification of the procedure of Iyer et al. [38,39]. The homogenate was layered on 4 mL of 0.85 M sucrose in 16 $\times$ 102 mm tubes and centrifuged for 45 Min at 85,000*g* in a SW 28 Ti rotor. The band at the interface was removed and resuspended in four parts of cold water. After 20 Min in the cold, it was centrifuged at 12,000*g* for 20 Min. The pellet was then resuspended in 0.32 M sucrose and recentrifuged as described, in order to obtain a highly purified myelin fraction.

2.6. Preparation of Samples for Western Blot Analysis

Sciatic nerves from adult rats, as well as cultured SC and subcellular fractions, were homogenized in lysis buffer [20 nM Hepes (pH 7.9), 350 nM NaCl, 20% glycerol, 1% NP-40, 1 mM MgCl2, 0.5 mM EDTA and 0.1 nM EGTA, 1 mM DTT, 0.1% PMSF, and leupeptin 10 μg/mL], sonicated and centrifuged at 15,000 rpm at 4 °C for 15 Min. The supernatant was stored at −80 °C and protein concentration was determined by the Bradford method [40,41].

Proteins (40 μg/lane) were separated by SDS-PAGE on 12.5% gels and electroblotted onto PVDF membranes. Nonspecific protein binding sites were blocked for 2 H at room temperature with blocking buffer containing 5% nonfat dry milk in PBS-Tween 20 0.1%. Rabbit anti-DMT1 (1:500) was the primary antibody used and peroxidase conjugated anti-rabbit IgG (1:10,000) was the secondary antibody. Immunocomplexes were visualized with the ECL Plus kit using a Storm 840 Phosphorimager (Molecular Dynamics) and analyzed using the Image Quant program. PC12 cell culture was run as a positive control in each experiment [42].

2.7. Immunocytochemistry

Seeded cells were cultured for 24 H and fixed with a solution of 4% (v/v) paraformaldehyde in PBS, pH 7.4, for 15 Min, and permeabilized with 0.2% (v/v) Triton X-100 in PBS. Nonspecific antigens were blocked with 5% (v/v) FCS in PBS for 2 H, followed by incubation with primary antibody overnight at 4 °C. Dilutions were as follows: mouse anti-S100β (1:200), mouse anti-Na^+/K^+-ATPase β1 (1:200), and rabbit anti-DMT1 (1:250). Cells were washed three times with PBS, incubated with Cy3 (1:1,000) or Cy2-conjugated secondary antibody(1:200) for 2 H, counterstained with Hoechst 32258 (2 μg/mL in PBS), mounted with Dako Fluorescent Mounting Medium, and examined using an Olympus BX50 epifluorescence microscope provided with a Cool-snap digital camera and an Olympus FV1000 confocal microscope.

To study the colocalization between the different cell markers, the overlap coefficient according to Manders (*R*) was estimated using the Image Pro Plus software (version 5.1) and a value higher than 0.6 was considered positive colocalization [43].

2.8. Preparation of Tissue Sections for Immunohistochemistry

Adult Wistar rats were deeply anesthetized (ketamine 75 mg/ kg i.p and xylazine 10 mg/ kg i.p.) and perfused through the heart with 200 mL of warm (37 °C) PBS followed by 100 mL of fixative (4% paraformaldehyde in 1 $\times$ PBS, pH 7.4) at 4 °C. The sciatic nerves were removed and post-fixed in the same solution overnight at 4 °C. The tissue was rinsed in 15% sucrose in PBS at 4 °C for at least 24 H and then rinsed in 30% sucrose in PBS and stored at −80 °C until processed. Tissues were cut into 16 μm sections with a cryostat (Leica) and the sections were mounted onto gelatin-precoated glass slides and stored at −20 °C.

The slides were rinsed twice in PBS and twice in PBS-Triton X-100 0.1%. After blocking in 5% FCS overnight at 4 °C, slides were incubated for 18–24 H in a humid chamber at 4 °C with S100β (1:100) and DMT1 (1:200) antibodies, diluted in PBS containing 1% FCS. Samples were rinsed three times in PBS and incubated at room temperature for 2 H with Cy3 (1:100) or Cy2 (1:100) secondary antibodies plus Hoechst 32258 (2 μg/mL in PBS) and later rinsed three times in PBS for another 5 Min each time. Sections were coverslipped with Dako Fluorescent Mounting Medium. Controls were done by incubation without the primary antibodies. The images were acquired both using an Olympus BX50 epifluorescence microscope provided with a Cool-snap digital camera or an Olympus FV1000 confocal microscope, and were analyzed as described above in Immunocytochemistry.

2.9. RNA Preparation

Total RNA was extracted from adult rat sciatic nerves using TRIZOL reagent and was purified according to the manufacturer's instructions. Cultured newborn or embryonic SC were lysed with lysis buffer RLT; afterwards total RNA was isolated using the RNeasy kit following the manufacturer's instructions [44].

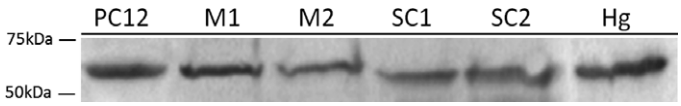

FIG 1 *Presence of DMT1 in samples isolated from rat sciatic nerves detected by Western blot analysis. PC12 (pheochromocytome cell line) as a positive control; Hg: sciatic nerve homogenate from adult rats; M1 and M2: purified myelin isolated from adult rat sciatic nerves; SC1 and SC2: cultured SC isolated from newborn rats. M1, M2, SC1, and SC2 each represent two independent experiments.* n = *4*

2.10. RT-PCR

RNA content was assessed by absorbance at 260 nm and its purity was determined by the ratio A260/ A280. Two μg of RNA were incubated with 1 μg oligo-dT primers for 5 Min at 70 °C. The reverse transcription (RT) took place for an hour at 42 °C in 25 μL of the following mixture: 1 × buffer, 5 mM DTT, 10 mM dNTPs, and 200 units of M-MLV reverse transcriptase. The reaction product was stored at −20 °C. PCR amplification was performed in 50 μL of the following mixture: 1 × PCR buffer, 1.25 units of Taq DNA polymerase, 25 mM $MgCl_2$, 10 mM dNTPs, and 200 ng/μL specific primers. The mixture was prepared before adding 1 μL cDNA. Primer sequences for DMT1 were as follows: forward: 5′- TTT TTG GCT TTC TCA TCA CTA TCA TGG CCC-3′ and reverse: 5′- ATT GGC TTC TCG AAC TTC CTG CTT ATT GGC −3′. Aliquots were taken after 40 PCR cycles product. The amplification products were expected to give a 251 pb fragment and were run on 1–1.5% agarose gels and visualized with ethidium bromide. The conditions of amplification were 1 Min at 94 °C, followed by 40 cycles of denaturation (94 °C, 1 Min), annealing (64 °C, 1 Min), and extension (72 °C, 1 Min), followed by a final extension at 72 °C for 10 Min. Reactions without template cDNA were run as negative controls and cDNA, obtained by RT from PC12 cell culture, was run as a positive control in each experiment [42].

3. Results

3.1. DMT1 Detection in the PNS

To demonstrate the presence of DMT1 in the PNS, we identified a 64-kDa band by Western blot analysis in tissue homogenate, in purified myelin isolated from adult rat sciatic nerves, and in cultured SC isolated from newborn rat sciatic nerves (Fig. 1). The apparent molecular weight of this band corresponds, in size, to the DMT1 band previously described in PC12 cells [42], which are used as a positive control.

3.2. DMT1 Detection in Cultured SC

To confirm the presence of DMT1, immunocytochemical assays were performed in cultured SC isolated from newborn rat sciatic nerves (Fig. 2). Panel A shows the presence of DMT1 while panel B confirms cells to belong to the SC lineage through positive testing for S100β −a SC marker present all along SC progeny. Panel C shows the immunostaining of cell nuclei by Hoechst. The merged image shows a clear colocalization of both markers (Fig. 2D), as confirmed by Mander's coefficient $R = 0.849$.

3.3. DMT1 Detection in Sciatic Nerve Sections

Finally, in order to assess the expression of DMT1 *in vivo,* immunohistochemical analyses were performed on adult rat sciatic nerves. Yet again, DMT1 is expressed in adult rat sciatic nerves as shown in longitudinal and cross sections (Figs. 3 and 4). The longitudinal section shows protein expression along the nerve fiber, where S100β is again used as a SC marker (Fig 3B); a clear colocalization of S100β and DMT1 (Fig. 3D) is confirmed by Mander s coefficient $R = 0.858$. Figure 4 shows the presence of DMT1 and S100β in a cross-section of rat sciatic nerve; the merge image shows these markers to colocalize with a value of $R = 0.923$ for Mander'ls coefficient (Fig. 4D). In order to distinguish immunofluorescence associated with SC and axons, Figure 5 shows how SC wrap the bundles of axons (positive for NF-200) while not colocalizing with them. When comparing Fig. 4 with Fig. 5, it is clear that DMT1 is expressed in SC, although we cannot rule out the possibility of its presence in axons.

3.4.Expression of DMT1 mRNA

On the basis of previous results, experiments were performed to detect DMT1 mRNA by RT-PCR analysis in the SC developmental lineage. Results show the presence of a 250 kb band that corresponds to the expected amplification fragment.

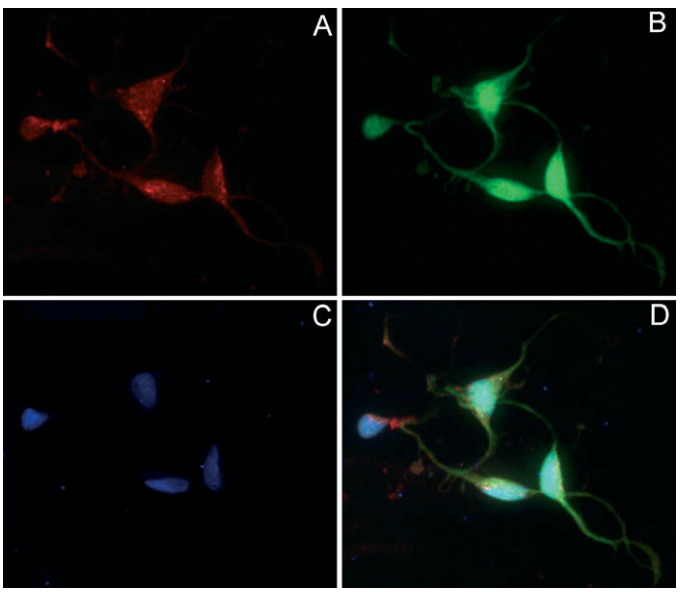

FIG 2 *DMT1 detection in cultured SC. Immunofluorescence study of the following markers: (A) DMT1, (B) S100β, (C) HOECHST nuclear staining, and (D) Merged (×60).* n = *4*

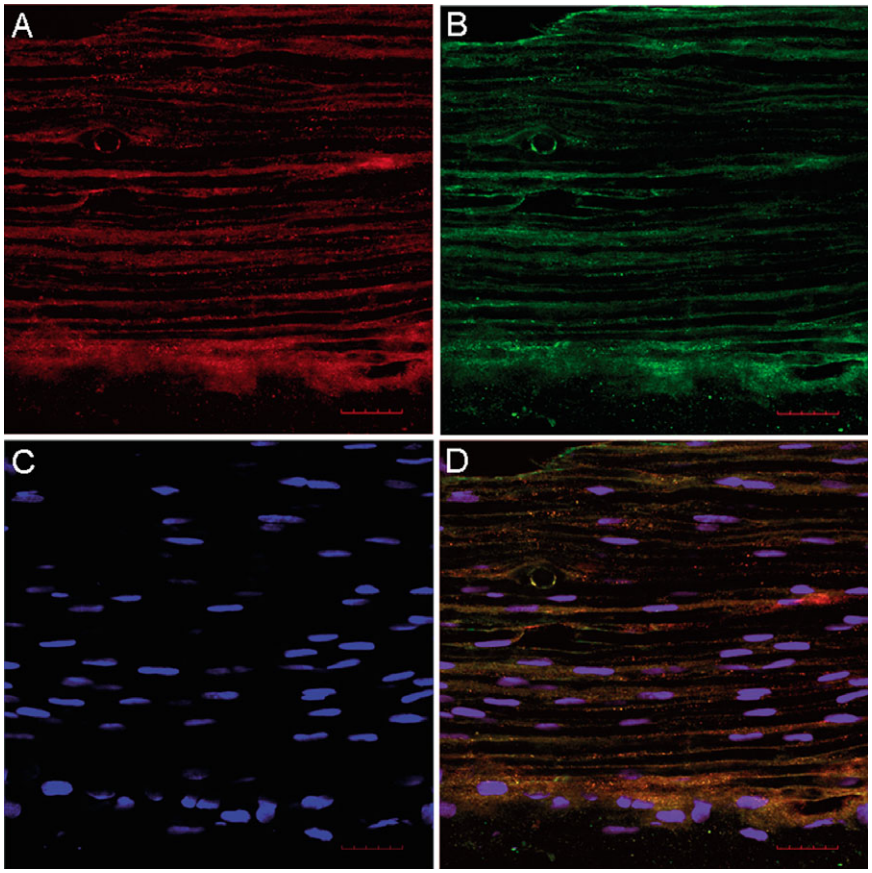

FIG 3 *DMT1 detection in longitudinal sections of control sciatic nerves. Immunofluorescence analyzed by confocal microscopy study: (A) DMT1, (B) S100β, (C) HOECHST nuclear staining, (D) Merged (×60).* n = *4*

DMT1 mRNA is detected in sciatic nerve from adult rats and all along SC progeny–SC precursors (E14-15), immature SC (E16, 18, and 20), and mature SC (P4) (Figs. 6 and 7).

3.5. Subcellular Localization of DMT1

To evaluate whether DMT1 is present in the PM of SC, we carried out confocal microscopy studies in isolated cultured cells using Na^+/K^+-ATPase as marker. Results illustrated in Fig. 8A hint at the presence of DMT1 in the plasma membrane, as shown by Na^+/K^+-ATPase immunoreactivity. This finding is confirmed through the use of subcellular fractionation and the detection of DMT1 in the PM fraction, which reinforces its role as a transporter in NTBI uptake (Fig. 8B). Nevertheless, its location in alternative subcellular fractions—such as the nucleus—deserves future studies.

4. Discussion

One of the most striking features of mature SC is their plasticity, which is essential in PNS remyelination. This property is clearly seen in the dedifferentiation of both myelinating and non-myelinating SC, which occurs after axotomy, mechanical crush or in neuron-free SC cultures. Under these circumstances, SC acquire a phenotype that is in many ways similar to that of immature SC during development [45,46].

We have previously demonstrated that iron, both as ferric ammonium citrate (FAC) and hTf, prevents SC dedifferentiation promoted by serum withdrawal through an increase in cAMP and CREB phosphorylation levels; this was shown to be an essential step in the expression of myelin proteins and a key element in SC maturation [28,29]. The observations made on cultured SC after iron treatment raised the question of how iron elicits its prodifferentiating effect in the absence of Tf.

Inorganic iron exists in two different redox states. The first one, ferric iron (Fe^{3+}), is insoluble at physiological pH values, so it must be bound to a carrier in order to be solubilized and then transported through cellular compartments. The second one, ferrous iron (Fe^{2+}), is soluble at physiological pH levels but is rapidly and spontaneously oxidized to ferric iron. Therefore it must be continuously reduced or bound to a carrier, which prevents the exposure of iron to oxygen, and the consequent free radical production.

Most iron is transported in plasma bound to Tf. Tf delivers iron to cells via a classical high-affinity low-capacity system, which has been extensively characterized [47,48]. However,

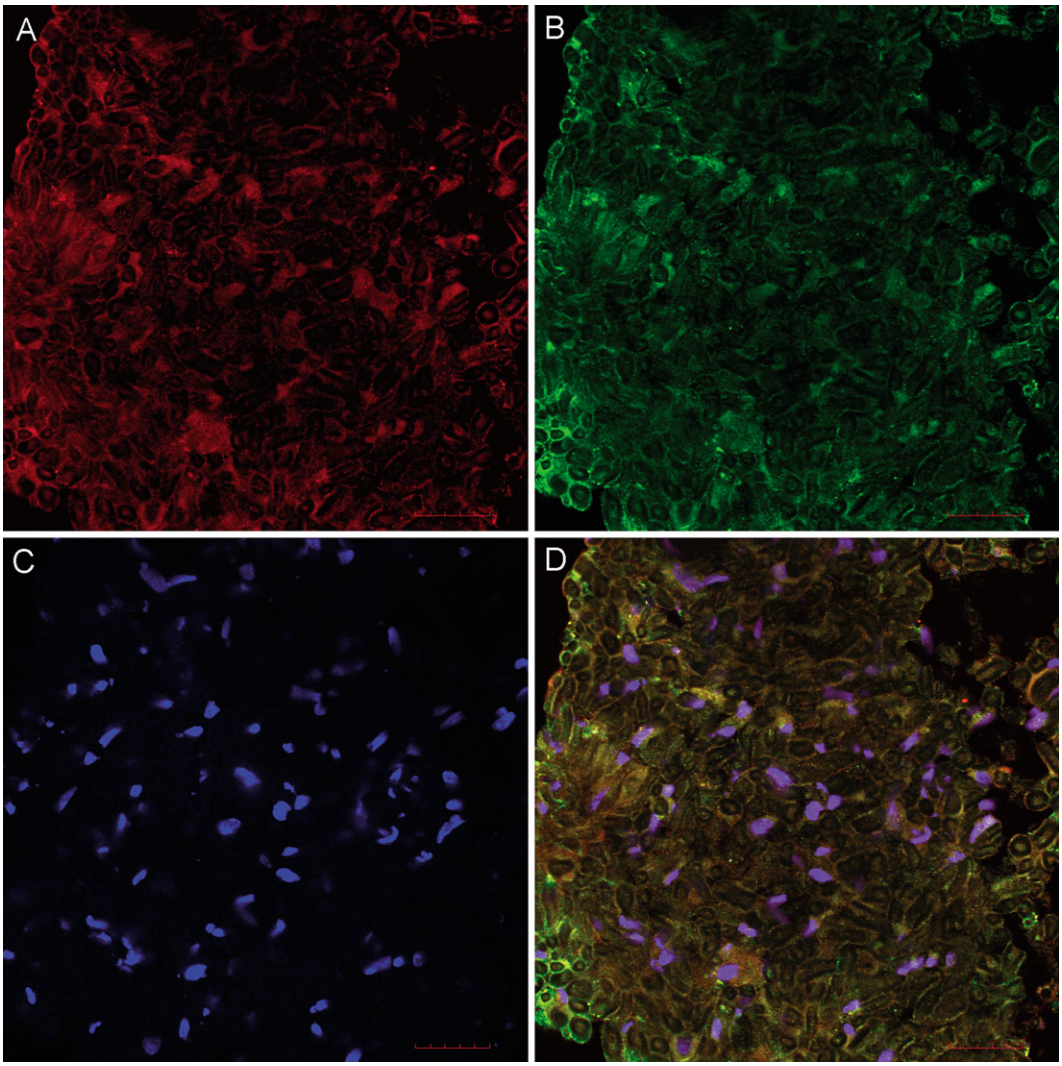

FIG 4 *DMT1 detection in cross-sections of control sciatic nerves. Immunofluorescence analyzed by confocal microscopy study: (A) DMT1, (B) S100β, (C) HOECHST nuclear staining, and (D) Merged (×60).* n = *3*

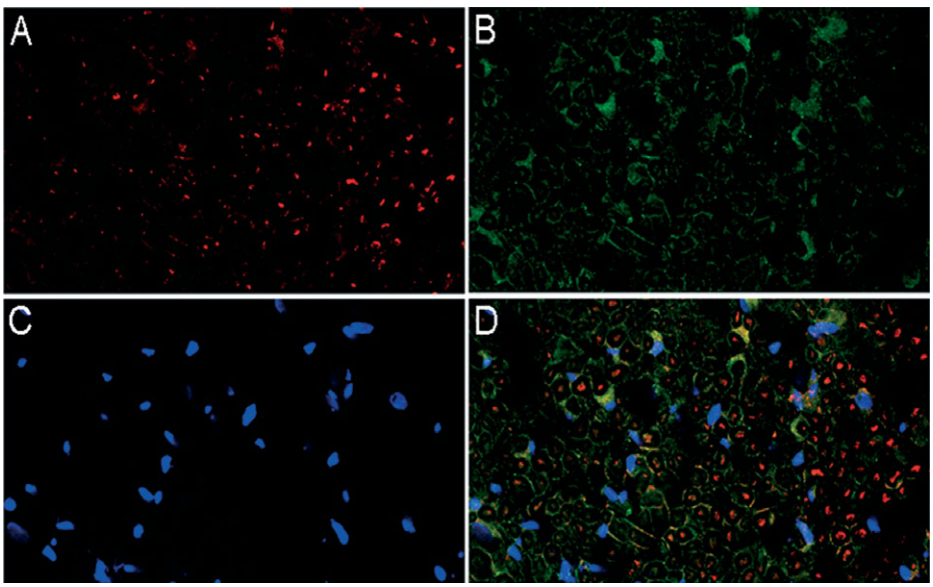

FIG 5 *SC and axon marker distribution in cross-sections of control sciatic nerves. Immunofluorescence analyzed by confocal microscopy study: (A) NF-200, (B) S100β, (C) HOECHST nuclear staining, and (D) Merged (×60).* n = *3*

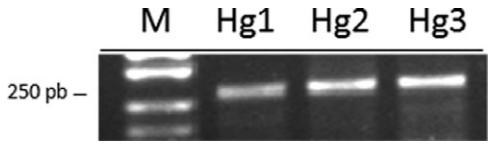

FIG 6 *mRNA expression of DMT1 in rat sciatic nerves. RT-PCR analysis of DMT1 mRNA in sciatic nerve homogenate (Hg). M =marker, Hg1, Hg2, Hg3 each represent three independent experiments.* n = *4*

the existence of NTBI uptake has been demonstrated in different experimental circumstances, and data on hypotransferrinemic animals show that brain iron uptake may be constitutive and independent of plasma Tf, Tf saturation, or regional brain iron concentration [49–51]. Taken together, these results have given impulse to the idea that specific alternative proteins might facilitate and regulate NTBI uptake. DMT1 is among these proteins.

Tf-free iron uptake into glial cells such as astrocytes proves the existence of an alternative DMT1-mediated uptake mechanism in the CNS [51–53], although no reports on this protein's expression have been available so far in the PNS. Here we demonstrate the presence of DMT1 all along the sciatic nerve, as well as in cultured SC, and its localization in the plasma membrane. It is worth pointing out, that DMT1 mRNA is present all along SC lineage.

Reports have suggested that iron is involved in the regenerating mechanisms that follow sciatic nerve injury; for instance, expression of TfR in motoneurons is increased after axotomy and during regeneration [54]. Furthermore, although no TBI uptake is found in the naive nerve, TfR immunoreactivity is observed 3 days post injury at the site of the trauma and in the distal part of the crushed sciatic nerve, where most of the immunostaining is localized in Büngner bands of denervated SC [27]. Accordingly, we have demonstrated the presence of Tf mRNA in SC isolated from crushed sciatic nerves, yet, no Tf mRNA is available in uninjured animals [44]. From the evidence discussed so far, it seems clear that there is a relationship between iron uptake and neural regeneration.

Our previous work has demonstrated the role of iron in SC maturation [29], while other studies have proven that decreased iron availability is strongly associated with hypomyelination caused by altered metabolic activity in olg [11]. On

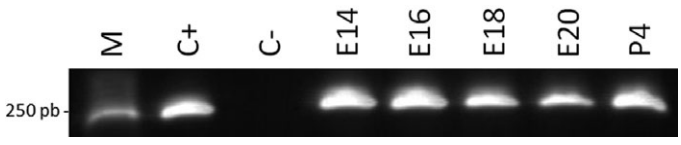

FIG 7 *mRNA expression of DMT1 in SC progeny. RT-PCR analysis of DMT1 mRNA in isolated SC of different maturational stages: M = Marker, C+ = positive control, C– = negative control, E14, E16, E18, E20 = 14, 16, 18, 20-days-old rat embryos, respectively, and P4 = postnatal day 4.* n = *3*

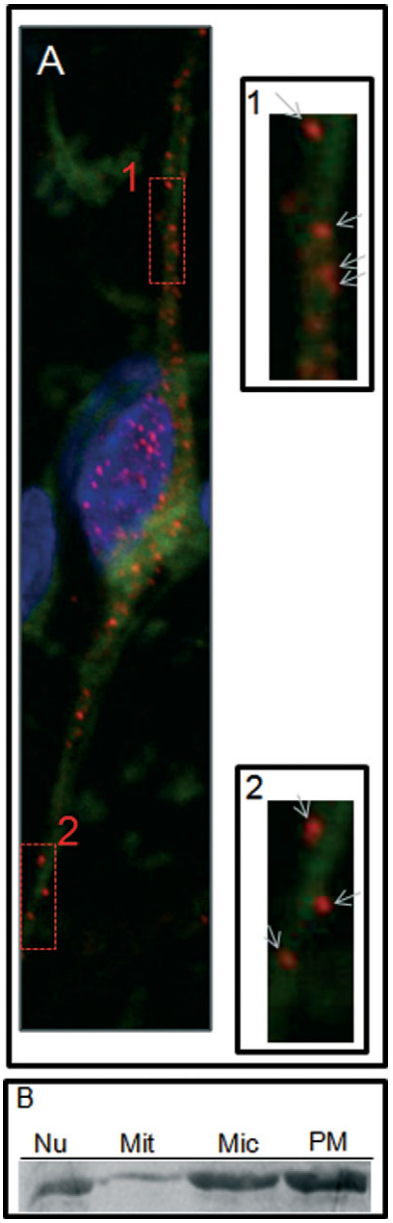

FIG 8 *Subcellular localization of DMT1. A: Immunocytochemical analysis of DMT1 (red) and Na^+/K^+-ATPase (green) through confocal microscopy. Immunostaining of cell nuclei with Hoechst (blue) (×60 + ×3), arrows show DMT1 immunoreactivity. 1 and 2 show higher magnification of representative areas,* n = *3. B: Western blot analysis of DMT1 in subcellular fractions from rat sciatic nerve: nuclei (NU), mitochondrial fraction (MIT), microsomal (MIC) and plasma membrane (PM) fraction.*

the whole, this evidence shows that the importance of iron in numerous processes regarding the production of myelin should not be understated [23].

Summing up, our results showing iron prodifferentiating effect may suggest its collaboration in SC plasticity, while current results showing DMT1 expression in SC progeny lead us

to postulate DMT1 involvement in ensuring the provision of iron essential for myelination in the PNS.

References

[1] Drapier, J. C. and Hibbs, J. B. Jr. (1986) Murine cytotoxic activated macrophages inhibit aconitase in tumor cells. J. Clin. Invest. 78, 790–797.

[2] Lill, R., Dutkiewicz, R., Elsasser, H. P., Hausmann, A., Netz, D. J., et al. (2006) Mechanisms of iron–sulfur protein maturation in mitochondria, cytosol and nucleus of eukaryotes. Biochim. Biophys. Acta. 1763, 652–667.

[3] Rouault, T. A. and Tong, W. H. (2005) Opinion: iron–sulphur cluster biogenesis and mitochondrial iron homeostasis. Nat. Rev. Mol. Cell Biol. 6, 345–351.

[4] Connor, J. R. and Menzies, S. L. (1996) Relationship of iron to oligodendrocytes and myelination. Glia 17, 83–93.

[5] Zucca, F. A., Giaveri, G., Gallorini, M., Albertini, A., Toscani, M., et al. (2004) The neuromelanin of human substantia nigra: physiological and pathogenic aspects. Pigment Cell Res. 17, 610–617.

[6] Crichton, R. R., Dexter, D. T., and Ward, R. J. (2008) Metal based neurodegenerative diseases—from molecular mechanisms to therapeutic strategies. Coord Chem. Rev. 252, 1189–1199.

[7] Burdette, S. C. and Lipard, S. J. (2003) Meeting of the minds: metalloneurochemistry. Proc. Natl. Acad. Sci. U.S.A. 100, 3605–3610.

[8] Crichton, R. R. and Ward, R. J. (2009) Iron Metabolism: From Molecular Mechanisms to Clinical Consequences, 3rd edn. John Wiley and Sons, Chichester, West Sussex, UK.

[9] Coe, C. L., Lubacha, G. R., Bianco, L., and Beard, J. L. (2009) A history of iron deficiency anemia during infancy alters brain monoamine activity later in juvenile monkeys. Dev. Psychobiol. 51, 301–309.

[10] Beard, J. L., Wiesinger, J. A., and Connor, J. R. (2003) Pre- and postweaning iron deficiency alters myelination in Sprague-Dawley rats. Dev. Neurosci. 25, 308–315.

[11] Todorich, B., Pasquini, J. M., Garcia, C. I., Paez, P. M., and Connor, J. R. (2009) Oligodendrocytes and myelination, the role of iron. Glia 7, 467–478.

[12] Connor, J. R., Snyder, B. S., Beard, J. L., Fine, R. E., and Mufson, E. J. (1992) Regional distribution of iron and iron-regulatory proteins in the brain in aging and Alzheimer's disease. J. Neurosci. Res. 31, 327–335.

[13] Crichton, R. R., Dexter, D. T., and Ward, R. J. (2011) Brain iron metabolism and its perturbation in neurological diseases. J. Neural. Transm. 118, 301–314.

[14] Gakh, O., Park, S., Liu, G., Macomber, L., Imlay, J. A., et al. (2006) Mitochondrial iron detoxification is a primary function of frataxin that limits oxidative damage and preserves cell longevity. Hum. Mol. Genet. 15, 467–479.

[15] Gille, G. and Reichmann, H. (2011) Iron-dependent functions of mitochondria—relation to neurodegeneration. J. Neural Transm. 118, 349–359.

[16] Sadrzadeh, S. M., and Saffari, Y. (2004) Iron and brain disorders. Am. J. Clin. Pathol. 121 Suppl: S64–S70.

[17] Zecca, L., Youdim, M. B., Riederer, P., Connor, J. R., and Crichton, R. R. (2004) Iron, brain ageing and neurodegenerative disorders. Nat. Rev. Neurosci. 5, 863–873.

[18] Oski, F. A. and Honig, A. S. (1978) The effects of therapy on the developmental scores of iron-deficient infants. J. Pediatr. 92, 21–25.

[19] Beard J, Eds. (2004) Indicators of the iron status of populations: free erythrocyte protoporphyrin and zinc protoporphyrin; serum and plasma iron, total iron binding capacity and transferrin saturation; and serum transferrin receptor. Beard, J., ed. In: Assessing the Iron Status of Populations: Report of a Joint World Health Organization/Centers for Disease Control and Prevention Technical Consultation on the Assessment of Iron Status at the Population Level. pp 75–94. World Health Organization/Centers for Disease Control, Geneva.

[20] Erikson, K. M., Jones, B. C., and Beard, J. L. (2000) Iron Deficiency alters dopamine transporter functioning in rat striatum. J Nutr. 130, 2831–2837.

[21] Ortiz, E., Pasquini, J. M., Thompson, K., Felt, B., Butkus, G., et al. (2004) Effect of manipulation of iron storage, transport, or availability on myelin—composition and brain iron content in three different animal models. J. Neurosci. Res. 77, 681–689.

[22] Connor, J. R. (1994) Iron acquisition and expression of iron regulatory proteins in the developing brain, manipulation by ethanol exposure, iron deprivation and cellular dysfunction. Dev. Neurosci. 16, 233–247.

[23] Morath, D. J. and Mayer-Proschel, M. (2001) Iron modulates the differentiation of a distinct population of glial precursor cells into oligodendrocytes. Dev. Biol. 237, 232–243.

[24] Moos, T. and Morgan, E. H. (1998). Evidence for low molecular weight, non-transferrin-bound iron in rat brain and cerebrospinal fluid. J. Neurosci. Res. 54, 486–494.

[25] Munaim, S. I. and Mescher, A. L. (1986) Transferrin and the trophic effect of neural tissue on amphibian limb regeneration blastemas. Dev. Biol. 116, 138–142.

[26] Mescher, A. L., Conell, E., Hsu, C., Chetna, P., and Overton, B. (1997) Transferrin is necessary and sufficient for the neural effect on growth in amphibian limb regeneration blastemas. Dev. Growth Differ. 39, 677–684.

[27] Raivich, G., Graeber, M. B., Gerhmann, J., and Kreutzberg, G. W. (1991) Transferrin receptor expression and iron uptake in the injured and regenerating sciatic nerve. Eur. J. Neurol. 3, 919–927.

[28] Salis, C., Goedelmann, C. J., Pasquini, J. M., Soto, E. F., and Setton-Avruj, C. P. (2002) Holotransferrin but not apotransferrin prevents schwann cell de-differentiation in culture. Dev. Neurosci. 24, 214–221.

[29] Salis, C., Davio, C., Usach, V., Urtasun, N., Goitia, B., et al. (2012) Iron and holotransferrin induce cAMP-dependent differentiation of Schwann cells. Neurochem. Int. 61, 798–806.

[30] Jenkitkasemwong, S., Wang, C. H., Mackenzie, B., and Knutson, M. D. (2012) Physiologic implications of metal-ion transport by ZIP14 and ZIP8. Biometals 25, 643–655.

[31] Garrick, M., Dolan, K. G., Horbinski, C., Ghio, A. J., Higgins, D., et al. (2003) DMT1, A mammalian transporter for multiple metals. Biometals 16, 41–54.

[32] Garrick, M., Singleton, S. T., Vargas, F., Kuo, H. C., Zhao, L., et al. (2006) DMT1, Which metals does it transport? Biol. Res. 39, 79–85.

[33] Hubert, N. and Hentze, M. W. (2002) Previously uncharacterized isoforms of divalent metal transporter (DMT)-1: implications for regulation and cellular function. Proc. Natl. Acad. Sci. U. S. A. 99, 12345–12350.

[34] Simovich, M. J., Conrad, M. E., Umbreit, J., Moore, E. G., Heinsworth, L., et al. (2002) Cellular location of proteins related to iron absortion and transport. Am. J. Hematol. 69, 164–170.

[35] Malviya, A. N., Rogue, P., and Vincedon, G. (1990) Stereospecific inositol 1,4,5–32P-trisphosphate binding to isolated rat liver nuclei: evidence for inositol trisphosphate receptor-mediated calcium release from the nucleus. Proc. Natl. Acad. Sci. U. S. A. 87, 9270–9274.

[36] D'Antuono, C., Fernández-Tomé, M. C., Sterin-Speziale, N., and Bernik, D. L. (2000) Lipid-protein interactions in rat renal subcellular membranes: a biophysical and biochemical study. Arch. Biochem. Biophys. 382, 39–47.

[37] Fernández-Tomé, M. C., Speziale, E., and Sterin-Speziale, N. (2002) Phospholipase C inhibitors and prostaglandins differentially regulate phosphatidyl choline synthesis in rat renal papilla. Evidence of compartmental regulation of CTP: phosphocholine cytidylyl transferase and CDP-choline: 1,2-diacylglycerol choline phosphotransferase. Biochim. Biophys. Acta. 1583, 185–194.

[38] Iyer, S., Rowe-Rendleman, C. L., Bianchi, R., and Eichberg, J. (1996) Tyrosine phosphorylation of myelin protein P0. J Neurosci Res. 46, 531–539.

[39] Usach, V., Goitia, B., Lavalle, L., Martínez Vivot, R., and Setton-Avruj, P. (2011) Bone marrow mononuclear cells migrate to the demyelinated sciatic nerve and transdifferentiate into Schwann cells after nerve injury: an attempt at a peripheral nervous system intrinsic repair mechanism. J Neurosci Res. 89, 1203–1217.

[40] Bradford, M. (1976) Rapid and sensitive method for the quantitation of microgram quantities of protein utilizing the principle of protein-dye binding. Anal. Biochem. 72, 248–254.

[41] Noble, J. E., and Bailey, M.J.A. (2009) Quantitation of Protein. Methods Enzymol. 463, 73–95.

[42] Roth, J. A., Horbinski, C., Higgins, D., Lein, P., and Garrick, M. D. (2002) Mechanisms of manganese-induced rat pheochromocytome (PC12) cell death and cell differentiation. Neurotoxicology 23, 147–157.

[43] Zinchuk, V., Zinchuk, O., and Okada, T. (2007) Quantitative colocalization analysis of multicolor confocal immunofluorescence microscopy images: pushing pixels to explore biological phenomena. Acta Histochem. Cytochem. 40, 101–111.

[44] Salis, C., Setton, C. P., Soto, E. F., and Pasquini, J. M. (2007). The mRNA of transferrin is expressed in Schwann cells during their maturation and after nerve injury. Exp. Neurology. 207, 85–94.

[45] Jessen, K. R. and Mirsky, R. (2005) The origin and development of glial cells in peripheral nerves. Nat. Rev. Neurosci. 6, 671–682.

[46] Mirsky, R., Woodhoo, A., Parkinson, D. B., Arthur-Farraj, P., Bhaskaran, A., et al. (2008) Novel signals controlling embryonic Schwann cell development, myelination and dedifferentiation. J. Peripher Nerv. Syst. 13, 122–135.

[47] Hodgson, L. L., Qual, E. A., and Morgan, E. H. (1994) Receptor independent uptake of transferrin bound iron by reticulocytes. Arch. Biochem. Biophys. 308, 318–326.

[48] Umbreit, J. N., Conrad, M. E., Moore, E. G., and Latour, L. F. (1998) Iron absorption and cellular transport, the mobilferrin/paraferritin paradigm. Semin. Hematol. 35, 13–16.

[49] Beard, J. L., Wiesinger, J. A., Li, N., and Connor, J. R. (2005) Brain iron uptake in hypotransferrinemic mice: influence of systemic iron status. J. Neurosci. Res. 79, 254–261.

[50] Ueda, F., Raja, K. B., Simpson, R. J., Trowbridge, I. S., and Bradbury, M. W. (1993) Rate of 59Fe uptake into brain and cerebrospinal fluid and the influence thereon of antibodies against the transferrin receptor. J. Neurochem. 60, 106–113.

[51] Takeda, A., Devenyi, A., and Connor, J. R. (1998) Evidence for non-transferrin-mediated uptake and release of iron and manganese in glial cell cultures from hypotransferrinemic mice. J. Neurosci. Res. 51, 454–462.

[52] Tulpule, K., Robinson, S. R., Bishop, G. M., and Dringen, R. (2010) Uptake of ferrous iron by cultured rat astrocytes. J. Neurosci. Res. 88, 563–571.

[53] Lane, D. J. R., Robinson, S. R., Czerwinska, H., Bishop, G. M., and Lawen, A. (2010) Two routes of iron accumulation in astrocytes: ascorbate-dependent ferrous iron uptake via the divalent metal transporter (DMT1) plus an independent route for ferric iron. Biochem. J. 432, 123–132.

[54] Graeber, M. B., Raivich, G., and Kreutzberg, G. W. (1989) Increase of transferrin receptors and iron uptake in the regenerating facial motoneurones. J. Neurosci. Res. 23, 342–345.